How to Determine the Laser-Induced Damage Threshold of 2-D Imaging Arrays

by Christopher Westgate

doi: http://dx.doi.org/10.1117/3.2523509
PDF ISBN: 9781510626188
epub ISBN: 9781510626195
mobi ISBN: 9781510626201

Published by

SPIE Press
P.O. Box 10
Bellingham, Washington 98227-0010 USA
Phone: +1 360.676.3290
Fax: +1 360.647.1445
Email: Books@spie.org
Web: http://spie.org

Spotlight vol. SL47
Last updated: 28 February 2019

SPIE.

Table of Contents

SPIE Spotlight Series

Welcome to SPIE Spotlight eBooks! This series of tutorials is designed to educate readers about a wide range of topics in optics and photonics. I like to think that these books address subjects that are too broad for journal articles but too concise for textbooks. We hope you enjoy this eBook, and we encourage you to submit your ideas for future Spotlights online.

Robert D. Fiete, *Series Editor*
Harris Corp.

Editorial Board

Preface

This Spotlight is intended for experimentalists learning how to perform laser damage measurements on cameras. The importance of understanding the laser-induced damage threshold of a camera and how it can define protection measures is discussed. A guide to the experimental methodology and testing considerations to measure the damage threshold of an off-the-shelf visible-band charge-coupled device (CCD) camera to a pulsed laser under laboratory conditions is presented. This same methodology can be applied to other 2-D detector arrays, and the steps to adjust the experimental process to perform continuous-wave laser damage threshold measurements are described. Finally, data analysis techniques relevant to this type of experiment are addressed.

1 Introduction

Two-dimensional (2-D) imaging arrays have made their way into countless applications, from industrial processes to medical imagery, area surveillance, and autonomous and remotely driven vehicles. The maturation of camera technology and the economies of scale have resulted in these sensors being widely implemented for every kind of task. They are relied on to perform critical safety roles, such as monitoring hostile areas or guiding heavy plant machinery, but they also complement our personal lives by enabling us to video-call our relatives or capture memories on our smartphones. The digital camera has found a home in almost every industry.

A camera sensor consists of two main components: a detector array and readout electronics. Modern visible-band cameras use a silicon photodiode array as the light-sensing medium. Figure 1 shows a cross-section of a single photosensitive element or "pixel" of a CCD camera. A photodiode consists of a junction between two layers of silicon: one is doped with a material with a lower valence than silicon, and the other one is doped with a material that has a higher valence than silicon. This results in one layer of electron-rich material and another layer with an abundance of holes, or a p-n junction. In a CCD pixel, a cathode is applied to the p-type layer, but an insulating layer is introduced between the n-type layer and the anode. In this way, the structure acts as a photocapacitor with the amount of charge stored per unit time being proportional to the light level. Individual pixels are arranged in a matrix to form a large photosensitive array.

Laser radiation can damage these sensitive 2-D imaging arrays even at long stand-off ranges because of the laser's highly collimated and coherent beam. In a focused camera system, the point source from a laser is brought to a single well-defined spot on the sensitive electronic array by the lens. The intensity of

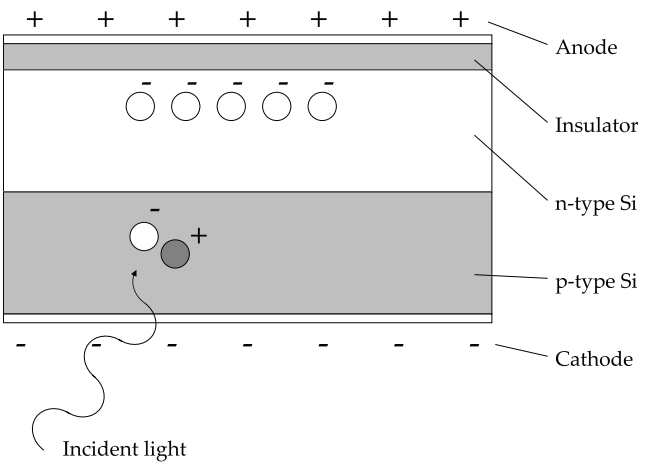

Figure 1 Cross-section of a single silicon CCD pixel active area.

laser light is referred to as fluence for pulsed laser sources (units of J cm^{-2}) or irradiance for continuous-wave (CW) lasers (in units of W cm^{-2}).

The focusing of light onto the array by the lens can be described in terms of optical gain, which is the ratio of irradiance at the pixel to the irradiance at the objective lens. This gain is often 10^6 or more (gain $\approx 10^6$ for $\lambda = 532$ nm, F-number = 8, and lens diameter = 25.4 mm). It is this high concentration of light by the lens that, given sufficient laser input, can damage the electronics by depositing enough energy to break electrical connections, fuse connections that should be isolated, or damage the material substrate itself.

The result of the physical damage to the sensing array caused by a laser can be effects such as reduced pixel output in response to a signal and bright or dark pixel damage. Bright or dark pixels can be generated singularly, in clusters, on lines of various sizes, or over the entire array. Figure 2 shows the laser damage to a visible-band CCD surveillance camera after exposure to pulsed green light at a range of 500 m.

High-power CW lasers are now commonplace in industry. Multiple kilowatts of CW laser power are used in industrial processing applications, such as metal

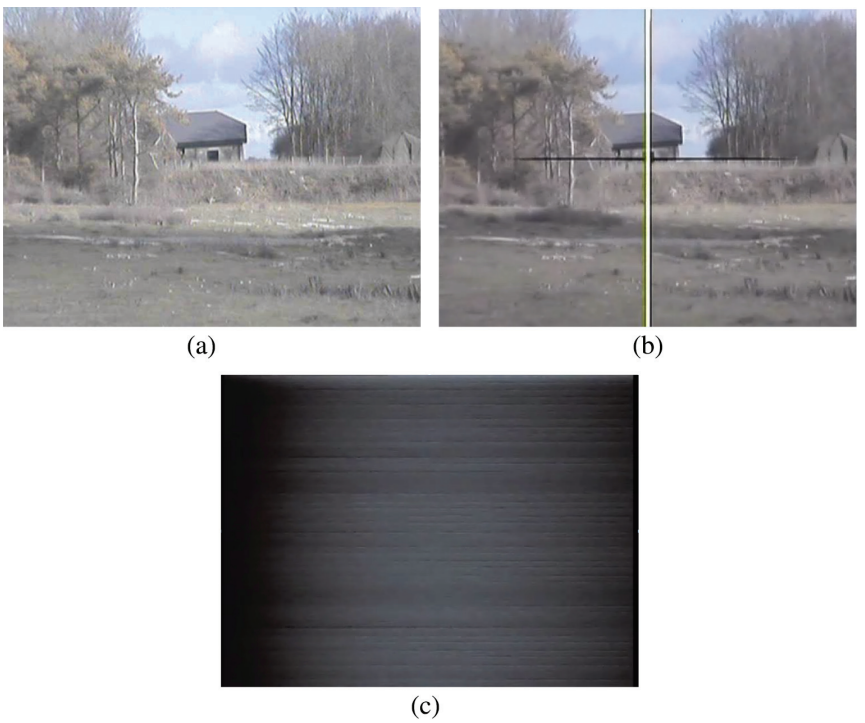

Figure 2 (a) Scene before laser illumination. A visible-band CCD images a scene and is illuminated by a pulsed laser system, causing (b) irreversible line damage and (c) full-frame damage. Total engagement time <1 s.

welding and cutting, and effective rust removal can now be achieved using portable, high-energy pulsed lasers. The specular component of a stray reflection from the work piece in such a process can direct laser radiation to a monitoring camera, which could be critical to safety. In the entertainment industry, stage performances with laser displays have caused documented cases of unintentional damage to cameras viewing the stage from the crowd.[1]

In the defence sector, the survivability of sensors can be mission critical. Self-damage from designators, rangefinders, and illuminators is currently the most common threat to a sensor, where the outgoing laser radiation is reflected back to the source, causing damage. Though less common, anti-sensor weapons also exist on the modern battlefield. An anti-sensor weapon known as a PAPV is one example; it uses a low-power laser to detect optics in the field and is coupled with a highly energetic laser pulse that can damage and potentially destroy the detected optical device.[2]

Commercially available, high-power CW handheld lasers [such as the 1-W laser shown in Fig. 3(a)] have been used to dazzle sensors, including the eye, and as they increase in power, their ability to cause damage inevitably follows. Figure 3(b) shows a 30-kW CW laser directed energy weapon (LDEW) aboard the USS Ponce.[3] The high power can structurally disable assets, such as unmanned aerial vehicles, but can also damage in-band sensors at far greater ranges due to the optical gain of the optics that focus the light onto the sensitive electronics of such sensors.

Protection measures for imaging sensors can be designed and implemented to protect against sensor damage and ensure that vital sensors remain functional, regardless of the industry or application. First, however, the laser-induced damage threshold (LIDT) of such devices must be accurately determined in order to set the requirements for these protective measures. Because of variations in sensor architecture and internal camera filters, the LIDT for a particular model of camera is often required, as opposed to assuming a laser damage threshold value for a

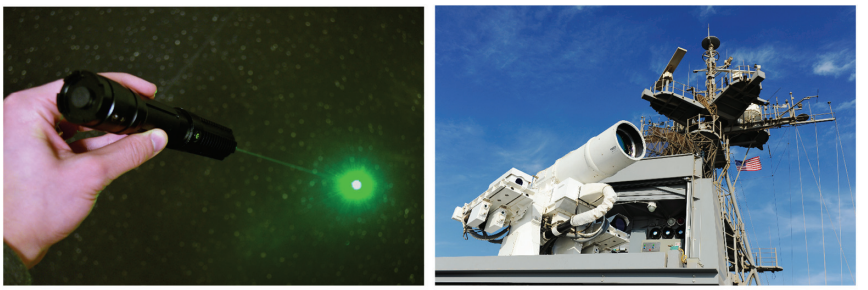

(a) (b)

Figure 3 Examples of CW lasers that can be encountered in civilian and military scenarios: (a) A commercially available 1-W CW hand held laser and (b) the 30-kW CW LDEW system on the USS Ponce (photo by John F. Williams, distributed under CC-PD-Mark license).

certain type of camera, i.e., silicon CCD. As the applications and proliferation of high-power lasers increase, the potential for damage to sensors increases. Quantifying the LIDT of a camera is, therefore, important so that the risk of damage to the sensor from a given laser source can be understood.

This Spotlight explains the methodology of establishing the LIDT of camera sensors to Q-switched (nanosecond pulse length) and CW laser sources with example images from visible-band cameras, but the techniques and methods can be expanded to other sensor architectures and wavebands.

2 Experimental Method

The experimental setup in its simplest form delivers a laser pulse into an objective lens that focuses the laser at the detector plane of the camera. The camera output is monitored after each laser event to check for permanent changes to the image caused by laser-induced damage. Morphological damage to the array itself is not directly studied in the scope of this experiment, only its symptoms, i.e., a change in digital output.

The radiant intensity at the detector plane, or fluence (in J cm^{-2}), can be calculated by dividing the energy into the camera by the beam area at the detector plane. In this Spotlight, all pulsed damage thresholds will be presented in terms of the fluence at the detector plane. The fluence threshold in the objective plane is the pixel plane threshold divided by the optical gain. Presenting LIDTs in terms of fluence at the detector has the benefit of being independent of the optics used. For example, for the same collected energy and focal length, the fluence at the focal plane will be higher when focused by an *F*/2 optic compared to an *F*/10 optic because the spot size at the focal plane for the *F*/2 optic will be smaller. Damage is caused by the laser fluence at the focal plane, not the total energy.

2.1 Experimental prerequisites

2.1.1 Optical setup overview

The laser input to the objective lens can be a beam that is directly emitted from the laser, or it can be expanded and collimated so that the beam is much larger than the objective lens. The beam directly emitted by the laser may contain significant aberrations that degrade its ability to be tightly focused; however, these aberrations can be significantly reduced by expanding the beam so that a smaller portion of the wavefront is sampled. This expansion and recollimation of the beam may be performed in the laboratory using two simple lenses designed as a beam-expanding telescope.

The subsampling of the expanded beam by the objective lens results in what is known as a top-hat beam and is representative of long-range laser illumination, where the beam has diverged and has become much larger than the collection

optic. For example, a laser propagating over a 1-km range with a typical divergence of 0.5 mrad gives a beam diameter of 50 cm, far greater than common objective-lens diameters, which normally range from millimeters up to several centimeters. This means the collected beam is approximately uniform (under low-turbulence conditions) across the lens aperture and focuses down to a diffraction-limited Airy disk. A Gaussian beam input is focused down to a Gaussian profile at the focal plane.

Figure 4 shows an example of an optical setup for an LIDT experiment. The laser should first go through a stage of energy control; in the diagram, two λ/2 waveplate polarizers are used in series to provide a large dynamic range of energies. Neutral density filters can be used instead, but they must be placed in a collimated beam section because the filters will need to be added and removed during the experiment to provide a range of energies, and if placed elsewhere, the filters will adjust the position of focus at the camera when added or removed. The use of a waveplate–polarizer combination negates this issue. After the energy-control stage, the raw laser output can simply be directed straight into the lens.

If simulating long-range illumination, the beam should first be expanded and recollimated such that the beam overfills the objective lens (recollimation can be easily verified using a shear plate interferometer).[4] The focal plane of the lens is where the camera under test (CUT) will be placed.

Pulsed laser damage thresholds are typically measured to single pulses. Some lasers can be triggered to fire single pulses; however, for certain lasers, it can be

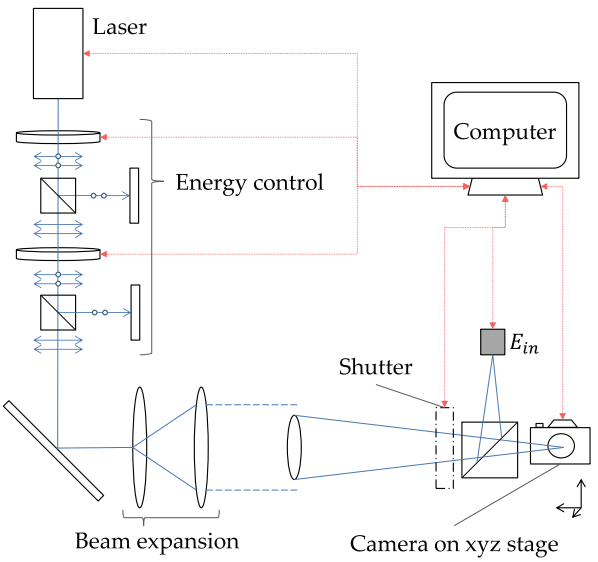

Figure 4 An example of an optical setup for assessing camera damage thresholds.

beneficial to allow the laser to fire repetitively and then use a pulse-picking shutter to let the desired number of pulses through to the camera for each event; this has the advantage of more stable pulse energies shot-to-shot. A pulse-picking shutter can be triggered from a laser output, such as a flashlamp synchronization pulse, so that the shutter opens for the next pulse only. Figure 5 shows the difference in stability for a flashlamp-pumped laboratory laser firing single shots every 5 s compared with single pulses that have been picked where the laser is firing repetitively at 10 Hz.

2.1.2 Determination of fluence at the camera

Energy into the camera

In order to measure the pulse energy into the camera, an energy pick-off in the form of an optical wedge or beamsplitter and energy-meter head should be used. The ratio between the energy from the pick-off and the energy to the CUT should be calibrated so that pulse-by-pulse energies to the CUT during the experiment can be measured.

Two energy-meter heads should be used: one at the reference pick-off location, and another at the CUT location. The energy meters should be sensitive to the laser wavelength, within the calibration date, and able to measure across the range of energies of interest. Ideally, the energy meters should be triggered by the source laser to ensure that the pulse energy for each exact pulse is captured. A range of energies between the lowest and highest anticipated levels should be recorded, and the linear relationship between E^{ref} and E^{camera} should be established. The energy meter at the CUT location can then be removed and the energy to the camera later inferred from the reference energy meter. A filter of known transmission can be placed in front of the reference energy meter to increase the

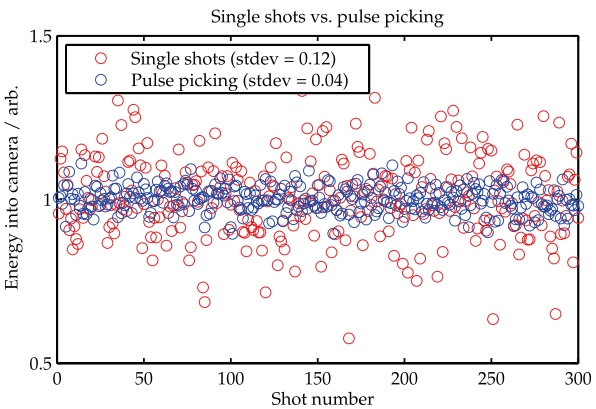

Figure 5 Single shots at a frequency of 0.2 Hz compared with pulse-picking single shots from the same flashlamp-pumped Nd:YAG laser running at 10 Hz.

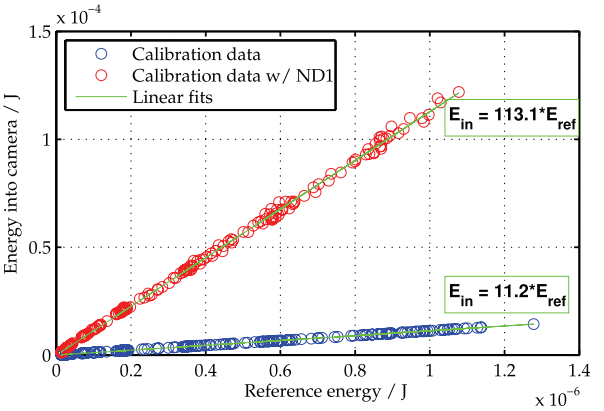

Figure 6 A calibration graph used to determine the energy into the camera for a reference energy meter with and without an absorbent filter covering placed in front of the energy meter.

energy to the CUT during testing without causing the reference meter to go out of range or become damaged.

Figure 6 shows typical calibration data for a reference energy meter by itself and with a neutral density filter with 10% transmission placed in front of it to protect the reference detector when operating above the detector's linear range.

Beam size at the focal plane

It is essential to take a real measurement of the beam size at the focal plane of the objective lens instead of determining the spot size through theory. Before the advent of digital beam profiling devices (BPDs), the beam size was measured using the knife-edge technique (Fig. 7). A straight edge (such as a razor blade)

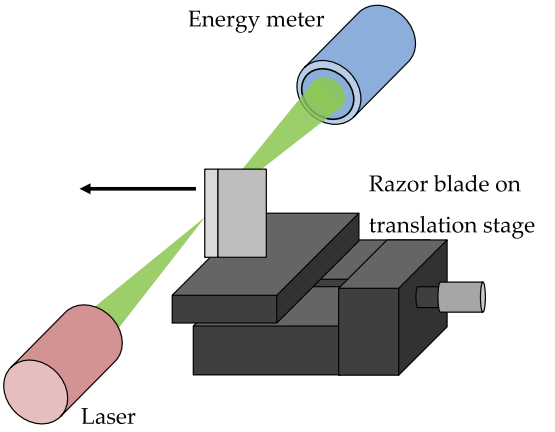

Figure 7 The beam size can be determined using the knife-edge method.

is held in a translation stage, and the blade is stepped perpendicularly across the beam. After each small step, an energy meter is used to measure the proportion of the beam that is blocked by the razor, and the resulting data are used to mathematically determine the beam size. In-depth papers on the mathematical fitting for this data can be found in the literature.[5,6] The disadvantage of the knife-edge scan is that it assumes the beam is sufficiently Gaussian and circularly symmetric. If the beam is not, the measured profile will not accurately represent the real intensity profile.

These days, digital BPDs, such as CCD profiling cameras, pinhole profilers, and scanning slit profilers, are easily available and relatively low cost. To measure the beam size using a CCD BPD, the device should be placed near the focus of the objective lens on an *xyz* translation stage and swept through the focus (i.e., toward and away from the laser along the beam path) until the optimum focus and smallest beam size is observed. For both Gaussian and Airy disk beam profiles, the central peak should be maximized in amplitude while minimizing the peak width.

The beam diameter is then usually taken as the full width at half maximum (FWHM) or the diameter at $1/e^2$ amplitude, although there are other methods of interpreting the beam size. When presenting any data, it is important to note which definition of beam size was used.

It follows naturally to consider using the CUT itself as a BPD. However, the CUT should have a sufficiently small pixel pitch to resolve the beam shape, and the laser must be attenuated to very low levels so that the CUT is not saturated. Even for slow optics and long wavelengths, an example camera with a pixel pitch of 3 μm may not give sufficient spatial resolution: at $F/22$ and 1064 nm, $r \approx 28.6$ μm. This gives a ±10.5% error in the spot width for this pixel size, which translates to a 22.1% error in area and, therefore, fluence. Because of this, a dedicated BPD with high spatial resolution is usually required to accurately measure the spot size.

Figure 8 shows the beam profile as seen by a BPD as it sweeps through focus, and optimum focus appears in subimage (d). Figure 9 shows the beam-width calculations graphically for the optimized beam profile used (inset image), where the line profile through the center of the beam is marked. If using a dedicated BPD, beam-diameter measurement tools are often part of the software that is included with the BPD.

In many situations, the intensity distribution at the focal plane will need to be magnified to enable a CCD profiler to sample it with adequate spatial resolution. Figure 10 shows an optical setup with relay optics that magnify the focal plane onto a permanently situated BPD. This optical setup has the advantage of measuring the spatial profile of the beam for every pulse and is especially useful for extending the use of this setup to outdoor testing where the distorted spatial profile of each pulse that has traveled through a turbulent atmosphere is captured. The CCD profiler in this configuration must be spatially calibrated to determine

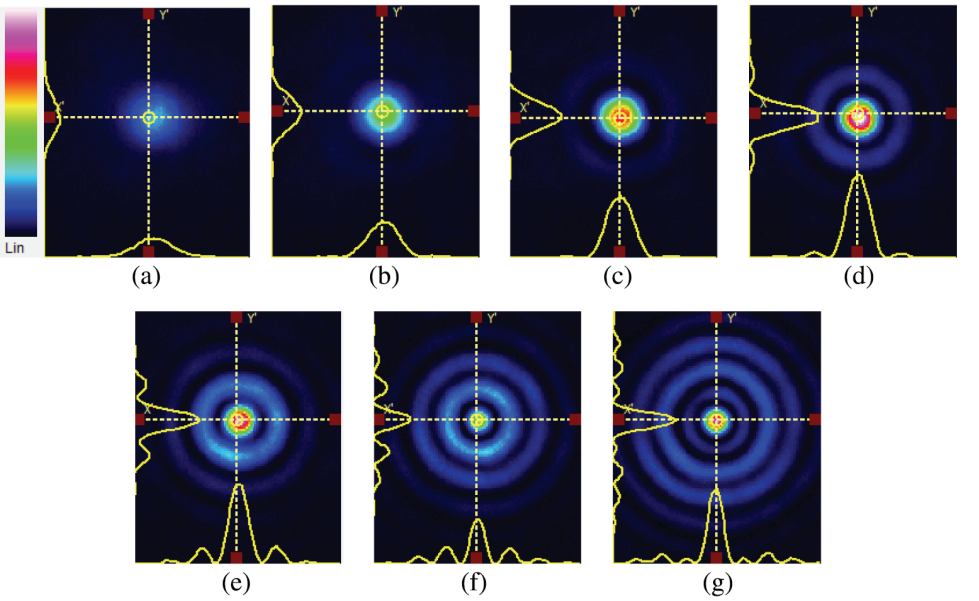

Figure 8 (a)–(g) A beam-profiling camera passing through focus. Optimum focus appears in image (d).

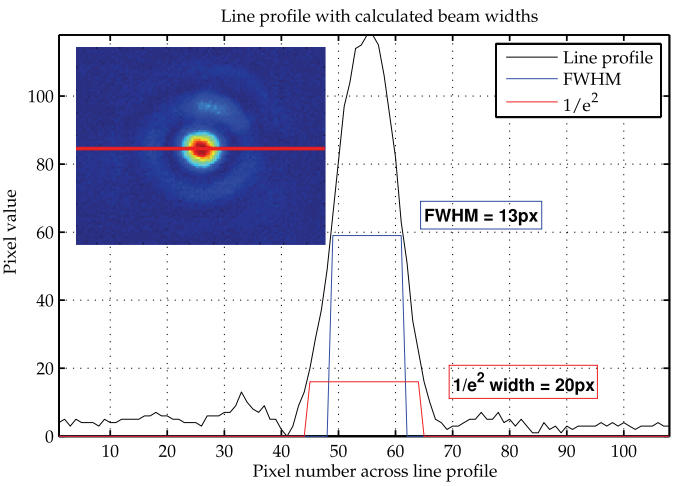

Figure 9 The values across the line profile are plotted, and the FWHM and $1/e^2$ beam widths are shown. Inset: a magnified and relay-imaged beam profile from a CCD beam-profiling camera, with the line profile (red) for analysis marked through the center.

the microns-per-pixel; this can be achieved by placing a grid of known size at the focal plane and imaging it. An example image recorded on the BPD is shown in Fig. 11. The grid is illuminated using a diffuse light source. Once calibrated,

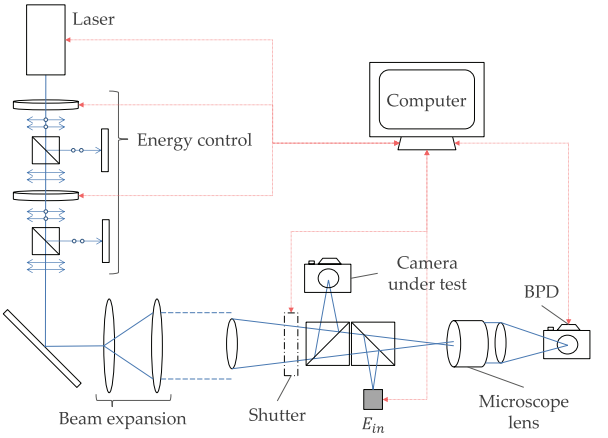

Figure 10 An example of an optical setup for assessing camera damage thresholds with a magnified focal plane at a permanently situated BPD.

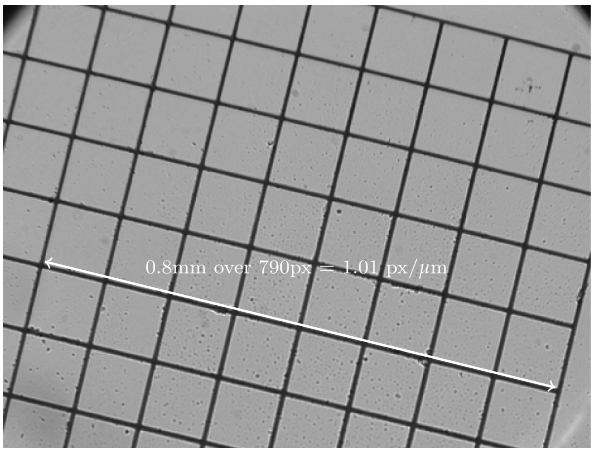

Figure 11 A magnified image from a BPD of a 0.1- × 0.1-mm^2 grid placed at the focal plane, used to spatially calibrate the BPD.

the magnified focal plane image can be used to determine the beam size on a shot-by-shot basis.

For interest, the measured spot size can be compared to theory. This is worth doing to check that the beam size is close to the theoretical size before proceeding with the experiment. The diffraction-limited spot diameter on the detector for a top-hat beam forming an Airy disk can be calculated using

$$d = 2.44F\lambda,$$

where d is the diameter of the spot up to the first dark ring, F is the F-number used ($F =$ focal length/beam diameter), and λ is the wavelength of the laser.

For Guassian input beams that focus down to a Guassian profile

$$d = 1.27F\lambda,$$

where d is the beam waist diameter up to the $1/e^2$ or 13.5% value.

In practice, the observed spot size is always larger than the theoretical diffraction-limited spot size. This is due to the Strehl ratio of the objective lens or lens system, which is defined as the ratio between the observed peak intensity and the peak intensity from a perfect system. Because a real lens has a Strehl ratio that is not unity, the focused beam spot will not be as small as that in theory and this will cause an overestimated fluence-at-focal-plane value if relying on theoretical values.

A typical Strehl ratio for a singlet lens can be as low as 0.3, and for an imaging quality lens, it can be >0.9. If the measured and theoretical sizes are close, taking into account the Strehl ratio of the lens, then confidence in the experimental setup is assured. The range of Strehl ratios highlights the importance of measuring the beam size at the focal plane as opposed to assuming the beam size from theory. Abberations in the laser beam itself may also be present, which can affect the beam's "focusability." Again, expansion and collimation of the input beam can help reduce these beam aberrations.

2.1.3 Focus of the camera

After measuring the spot size, the CUT is placed at the focal plane of the lens. The camera should be placed on an *xyz* translation stage, so that the focus can be adjusted (*z* axis), and the location of the laser's focal spot moved around the array (*xy* axes). The goal is now to move the CUT so that it is at the optimum focus to the laser, i.e., the same as when measured by the BPD. This is done in the same way as the BPD by moving the camera toward and away from the laser in order to sweep it through the focus, while observing the real-time output of the CUT. It is often helpful to trigger the camera from the laser during pulsed laser testing to ensure that each frame captures the laser beam. The camera is usually triggered from an output on the laser, such as the flashlamp synchronization pulse, and is useful when aligning and focusing the beam onto the sensor.

The laser energy should be minimized so that the camera is not saturated, allowing the user to accurately identify when the peak of the spot is brightest. If additional attenuating filters are required for the focusing process, they can be placed in collimated space, which allows them to be added and removed freely without affecting focus providing they are sufficiently flat. If they cannot be placed in collimated space, then they should be placed elsewhere (preferably where the beam size is large to reduce the intensity on the filters and avoid damaging them); and they should be left in for the duration of testing so that the focal position at the CUT does not change. Focus is found when the focal spot is smallest and brightest, i.e., the peak of focus is maximized.

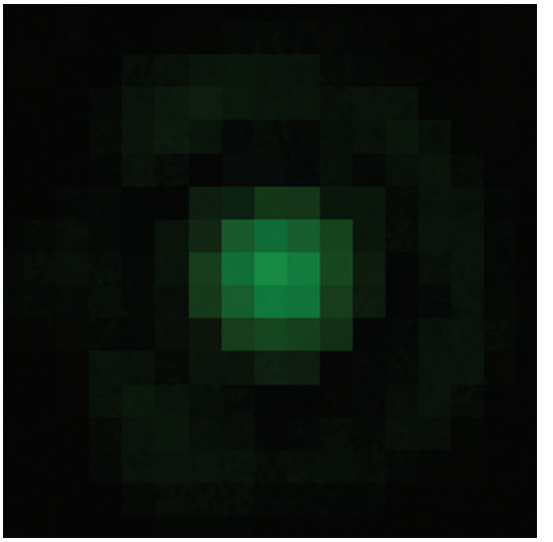

Figure 12 The output of a visible-band CCD camera with the (highly attenuated) laser focused on it.

Figure 12 shows the output of a CUT with an attenuated laser optimally focused onto it. Note the reduced resolution as a result of the pixel size; because of the resolution, a certain degree of experimentation with sweeping through focus may be required to convince the user that optimum focus is indeed achieved. For flashlamp-based lasers, care must be taken to not focus on the flashlamps themselves. To reduce the flashlamp-to-laser signal ratio, a notch filter at the laser wavelength can be placed before the CUT. Note that the filter itself will change the focal position, so it must again be left in for the duration of testing or placed in collimated space so that it can be removed after optimum focus is found.

2.2 Testing methodology

Before testing begins, the user should be able to view and record single pulse energies and the live output of the camera. The energy of each pulse should be understood through calibration of a reference energy meter, and the beam size of the laser at the focal plane should be determined. The camera should be placed at optimum focus to the laser.

A typical test is performed as below, starting from a low laser energy so that the CUT is not immediately damaged.

1. A single shot is fired at the camera. For every shot, the shot number, reference energy meter reading, and damage effect (no effect, single pixel, multi-pixel, line, and full frame) should be logged.

2. The output of the camera is checked for an effect. The sensor is covered to check for bright pixels and uniformly illuminated using an external light source to check for dark pixels.
   - If no effect is observed, the energy is increased.
   - If an effect is generated, the output of the camera is saved under a relevant file name (such as the shot number). The camera is translated diagonally (*xy* axes) so the next pulse can interact with fresh material, and the sensor is refocused.
3. Steps 1 and 2 are repeated until all the data required are collected. It is often useful to repeat shots several times if the damage effect is not consistent for a given input, for example, if some shots cause multi-pixel damage and others cause column damage. This occurs when the input is at the threshold for a certain type of damage, and more data points will define this threshold more clearly.

Light pixel damage is best observed when the scene is dark. Conversely, a light source, such as a flashlight, can be directed onto the sensor to check for any dark pixel damage. Figure 13 shows examples of light and dark pixel damage for (a) a color CMOS camera tested against a pulsed green laser and (b) an InGaAs camera tested against a CW IR infrared radiation (IR) laser. Translating the camera is important because a pulse interacting with an already-damaged spot can cause greater damage effects than if the pulse interacted with fresh material. The camera focus should be checked after translating the camera in case the translation stage is not mounted squarely to the input beam. Any small change in focus will reduce the fluence at the detector plane for a given energy, giving false negative results.

The test continues until the desired scale of damage is achieved and enough data points have been collected.

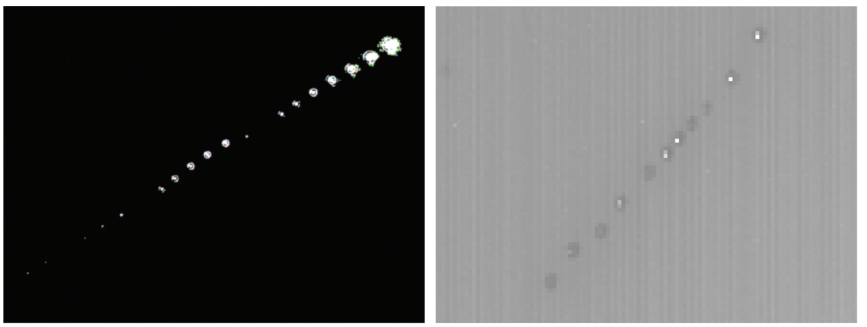

(a) (b)

Figure 13 The output images of two different arrays, showing light pixel damage (a) from pulsed laser testing and dark pixel damage (b) from CW laser testing. Note the diagonal translation between events.

2.3 Adaptation for a continuous wave

Establishing the LIDT of a camera to a CW laser exactly follows the aforementioned procedures, i.e., the power going into the camera and spot size must first be understood through calibration of a reference meter and measurement of the spot size. For CW exposures, a method for controlling the CW laser exposure time is also required. This can be in the form of a mechanical shutter; fast mechanical shutters can bring exposure durations down to milliseconds. To minimize the laser power "ramping" up and down as a result of the shutter paddle gradually revealing and concealing the beam as it opens and closes, the laser can be focused at the paddle. This reduces the beam size and, therefore, the time taken for the paddle to traverse the whole beam diameter. The beam can then be recollimated and focused after the shutter.

For faster exposures than can be achieved with a shutter alone, an easily modified spinning chopper can be used in series with a shutter (Fig. 14). Covering the slots of a chopper blade with tape and leaving one slot open allows the shutter-chopper device to generate a single short exposure, as shown by the timing diagram in Fig. 15. In any case, the temporal profile of the laser exposure should always be verified using a photodiode and oscilloscope.

3 Data Analysis

The interpreted LIDT depends on the definition of damage, which is often task dependent. For example, damage may mean small clusters for one application, whereas in other scenarios, single pixel effects may constitute damage. Three methods of presenting data collected from a LIDT experiment are described below.

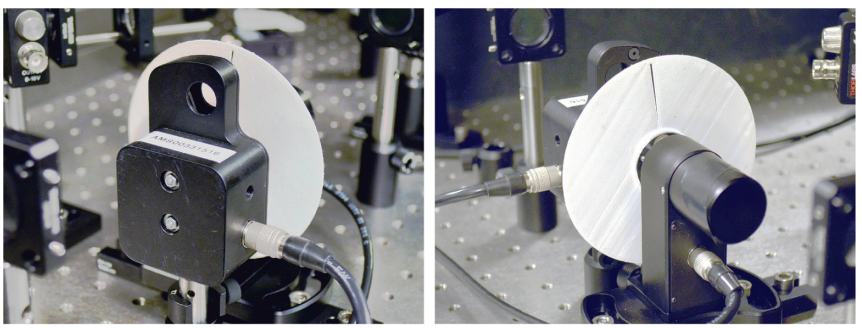

(a) (b)

Figure 14 A shutter-chopper combination used to generate shorter CW exposure lengths than can be achieved with a shutter alone. (a) Front and (b) back showing a 3-D printed chopper blade with one slot only.

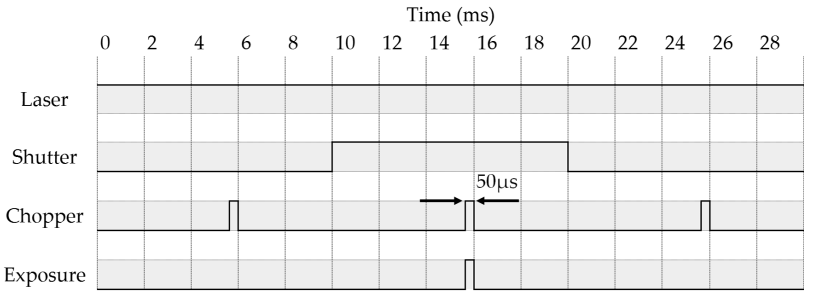

Figure 15 A timing diagram for a CW laser with 10-ms shutter and modified 10-kHz chopper with a single slot, achieving a single 50-µs exposure.

3.1 Basic presentation

The simplest presentation of LIDT data is a plot of damage "type" against input energy or fluence. This type of plot is useful to quickly identify step changes in damage scale, for example, between no damage and single pixel damage, or multiple pixel damage and row/column damage. An example is shown in Fig. 16. A shortfall of this quick and easy graph is that the scale of damage is not captured; small and large clusters of multiple pixel damage are presented equally and cannot be differentiated by this graph. Further data processing is required to attain more information.

If a task constitutes "damage" as line effects, then Fig. 16 indicates that the damage threshold is a focal plane fluence of 1.5 J cm^{-2}. Similarly, other tasks may have tighter tolerances and may define damage as single pixel effects; in these cases, the damage threshold would be 0.2 J cm^{-2}.

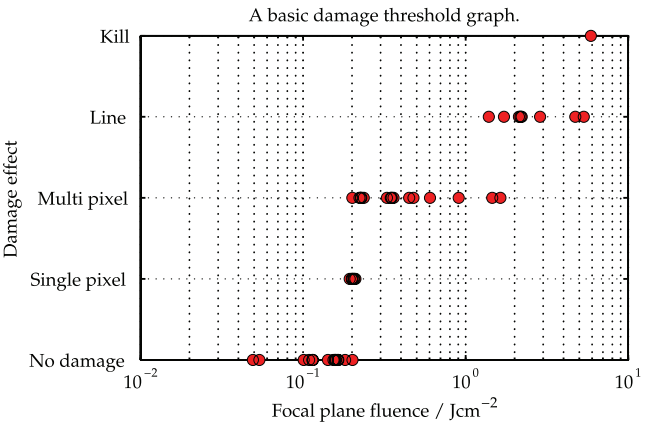

Figure 16 A simple laser damage plot of a typical visible-band monochrome CCD camera.

3.2 Pixel counting

A plot that shows the number of damaged pixels is useful for understanding exactly how much damage a given fluence will inflict; for cameras, which typically suffer only one type of damage, or one type of damage under a certain fluence, this type of plot can be combined with information about the lens system to estimate the amount of field of view that will be obscured by a damage spot. An example of this type of plot is shown in Fig. 17.

The saved output images from each shot that caused damage can be processed to count the actual number of pixels damaged. The processing can be done trivially using popular commercial software packages. The basic steps are explained below for processing images from a color camera that have bright pixel damage on a dark background:

1. The average background pixel value is first calculated, which allows the user to set a threshold value to differentiate bright pixels from the background.
2. A region of interest around the damage site is then selected by the user and the threshold value applied, generating three binary images from the red, green, and blue channels.
3. The three binary images are superimposed, and the resultant image is thresholded again to find the total number of pixels affected (Fig. 18).

For monochrome cameras, only one channel is output, so step 3 is not required and step 2 is simplified to create a single binary image, which is summed to find the total number of damaged pixels above the threshold level.

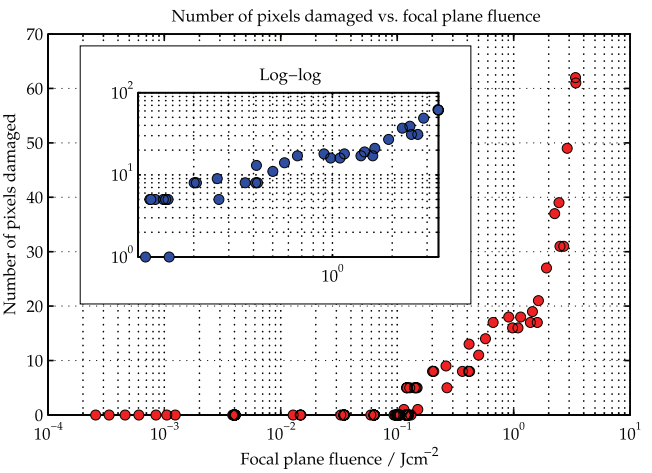

Figure 17 A more detailed plot showing the number of pixels damaged versus focal-plane fluence for a visible-band monochrome CCD camera (inset shows the same data on log–log axes).

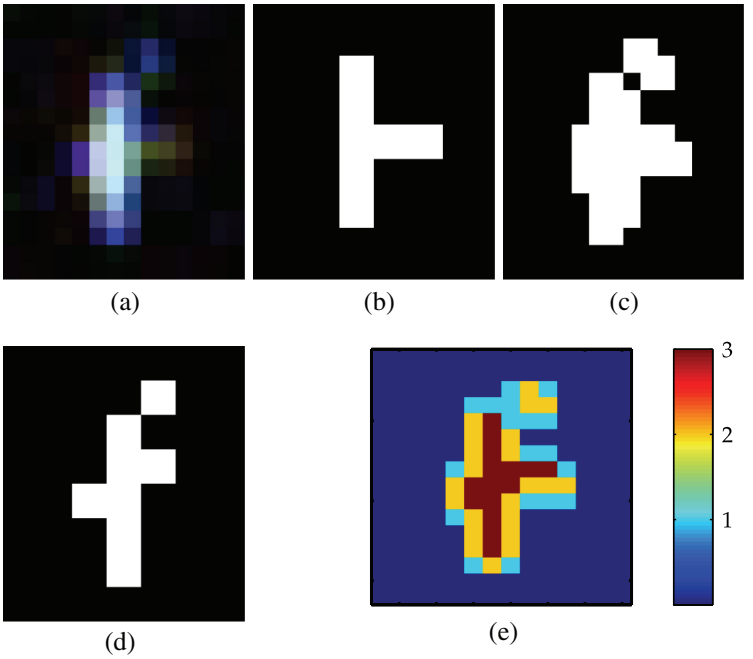

Figure 18 Image processing steps to determine the total number of pixels damaged: (a) Laser damage site, (b) red channel, (c) green channel, (d) blue channel, and (e) superimposed channels.

3.3 Probit fits

A probit fit can be applied to the data to generate values that indicate the fitted fluence value, where the probability of damage equals *x*%, called the FD*x* value. These values are indiscriminate to the level of damage (i.e., number of pixels) created for a given input energy. Probit fits can be applied easily to a dichotomous dataset by using built-in functions in commonly available commercial software (Fig. 19). The dichotomous datasets are created by compressing all occurrences of damage, whether they caused single pixel damage or more, into a value of "1" to indicate that damage occurred for a particular energy, and all occurrences of no damage to a "0."

A probit plot is also useful to estimate the change in damage probability if there is variance in input energy or focal-plane fluence caused by factors such as atmospheric turbulence or laser output instability. If the variance is known, then the range of expected input fluences can be used to estimate the change in damage probability. Figure 20 shows the FD^{50} focal plane fluence, i.e., the focal plane fluence that has a 50% chance of causing damage. By introducing a variance to the input fluence (purple lines), a range of damage probabilities is given.

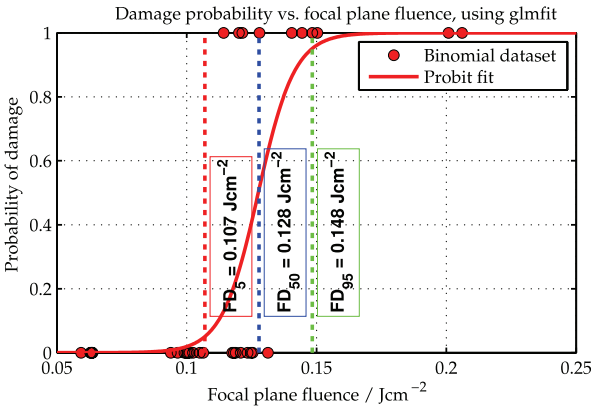

Figure 19 A probit fit plot applied to LIDT data.

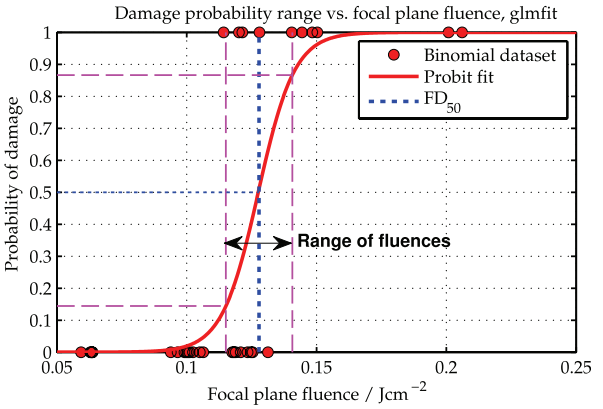

Figure 20 A probit fit plot applied to LIDT data with lines showing the resulting range of probabilities given a range of input fluences (purple lines).

4 Summary

This Spotlight has shown the steps required to perform a LIDT measurement, with experimental precautions for consideration and examples of presenting the data. Most importantly, the beam-size and energy calibrations should be done accurately, and the experiment operator should ensure the CUT remains in optimum focus throughout the test, particularly when the camera is translated.

There are many ways to perform a LIDT experiment, and often the experiment will require more optical elements than are shown in the simplified optics diagram shown in Section 2. There is no industrial standard method for determining the LIDT; however, if the damage threshold data are portrayed in terms of

intensity at the detector, this gives a universal number for others to use, and it can easily be recreated by others.

Once the LIDT of a detector of interest is quantified, the specifications for any future protection measures to prevent or limit damage can be defined.

References

1. D. Bickley, "Lasers take down a $20,000 camera in less than one second," 2013, https://fstoppers.com/news/lasers-take-down-20000-camera-less-one-second-2700.
2. Nudelman Precision Engineering Design Bureau (KBtochmash), "Portable laser automatic device of optronic countermeasure," http://kbtochmash.com/products-main/products-main_14.html (02 January 2018).
3. M. Peach, "US navy ship-mounted 30 kW laser weapon tested in Persian Gulf," 2014, http://optics.org/news/5/12/18.
4. J. Choi et al., "Wedge-plate shearing interferometers for collimation testing: use of a moire technique," *Appl. Opt.* **34**(19), 3628–3638 (1995).
5. J. M. Khosrofian and B. A. Garetz, "Measurement of a Gaussian laser beam diameter through the direct inversion of knife-edge data," *Appl. Opt.* **22**(21), 3406–3410 (1983).
6. M. A. de Araujo et al., "Measurement of Gaussian laser beam radius using the knife-edge technique: improvement on data analysis," *Appl. Opt.* **48**(2), 393–396 (2009).

Christopher Westgate received his bachelor's and master's degrees in biomedical engineering from Imperial College London. He is a senior research scientist at the Defence Science and Technology Laboratory, Porton Down. He uses his engineering knowledge and optics expertise to develop and assess innovative technologies for laser protection, and his roles as UK technical lead and technical partner to inform customers and stakeholders for the benefit of UK defense.